

# An Effective Two-time Scale Composite Control Contraction Based Chaotic Trajectory Tracking of Two-link Flexible Manipulator

Kshetrimayum Lochan, Asim Khan, Binoy Krishna Roy, Bidyadhar Subudhi,  
Lakmal Seneviratne, and Irfan Hussain\*

**Abstract**—In this paper, a two-link flexible manipulator  $n$ -dimensional model is developed using the assumed modes method. Based on this model, the manipulator dynamics are segregated into two subsystems by the two-time scale decomposition method of singular perturbation. Subsequently, a contraction-based control theory and a backstepping control of composite controller are investigated for the desired chaotic trajectory tracking along with tip deflection vibration suppression. In the two subsystems, the slow subsystem is involved in the modelling of the joint angles, and the fast subsystem is for corrected flexible modes of vibration suppression. In order to guarantee strict stability, Lyapunov's stability is realized for closed-loop system uniform boundedness. Thus, by choosing the control parameters appropriately, the system states converge to a neighborhood of asymptotic stability. Eventually, extensive validation by comparative simulations of the Quanser model of the two-link flexible manipulator is carried out to demonstrate and indicate the effectiveness of the proposed composite controller in terms of faster tip deflection vibration suppression and better trajectory tracking.

**Index Terms**—Flexible manipulators, assumed modes method, singular perturbation, contraction based theory.

## I. INTRODUCTION

Over the past few years, the direct application object of multibody system flexible dynamic analysis and control theory has been the flexible manipulators. As a result of its evident physical model and easily validated qualities, it has become an important issue in the areas of robotics, aerospace, aviation, medicines, education, etc. The flexible manipulator is comprised of complicated dynamics and the research area content is segregated into two directions, modelling of the flexible manipulators and controller design. The area of the control problems indicate the type of the controller designed for flexible manipulators. The angular and tip position deflection given by [1], angular and tip trajectory tracking problem discussed in [2], the regulation problem discussed in [3] are the commonly used control problems of two-link flexible manipulator (TLFM). The most challenging and the accepted control problem is based on the trajectory tracking

[2]. The goal of this study is to design a reliable control algorithm for the two-time scale subsystem employing a novel trajectory tracking problem for TLFM with quick tip deflection suppression using singular perturbation (SP).

The accurate operation of the flexible manipulator (FM) depends on the method of modelling and the control design. The methods of modelling in flexible manipulator are mainly the lumped parameter method (LPM) [4], assumed modes method (AMM) [2] and finite element method (FEM) [5]. AMM is the most commonly used modelling method for the flexible manipulators. The singular perturbation (SP) technique [6] is mostly used in coordination with AMM for the designing of controllers. In this techniques, separation decomposition method of two-time scale division is done for the segregation of two subsystems. One subsystem is segregated as slow dynamics from the original dynamics and the other as the fast dynamics. To achieve desired performances, separate controllers are designed for separate control inputs. Many methods of modeling are enlisted for the fast suppression of the link's deflection [7]. Hence, singular perturbation method is most appropriate in links deflection suppression as it entails controllers that can be designed in terms of slow and flexible dynamics. In the literature, some control techniques for slow subsystem have been reported like PID feedback control [8], PID ANN [7], fuzzy non-singular TSMC [9], inverse dynamic based control [10] of trajectory tracking. Similarly, PID [8], LQR based state feedback control [11], Lyapunov based control [10] are designed for the tip deflection suppression of fast subsystem. In this paper, a desired trajectory chaotic signal generated from a chaotic system is utilized as the desired trajectory. For achieving the expected trajectory, a contraction theory based controller is used for the slow subsystem. A good trajectory tracking performance is observed with this controller with less steady state error. The technique of backstepping control is designed for fast tip deflection suppression. The error dynamics are also given with respect to the tip deflection and desired trajectory. With this, using theory of Lyapunov stability, it guarantees the stability of the dynamics in terms of convergence of the error dynamics. The design of Genesis-Tesi chaotic trajectory tracking with contraction based theory along with backstepping controller for the subsystems is hardly seen in the literature for controlling a TLFM.

The rest of the paper is organised as follows. The dynamics of the two-link flexible manipulator is presented in Section II, Section III describes the slow and fast subsystems via singular perturbation. Section IV describes the composite

Kshetrimayum Lochan, Asim Khan, Lakmal Seneviratne, and Irfan Hussain are with the Department of Mechanical Engineering, Khalifa University Center for Robotics and Autonomous Systems (KUCARS), Khalifa University, United Arab Emirates. lochan.kshetrimayum@ku.ac.ae, asim.khan@ku.ac.ae, lakmal.seneviratne@ku.ac.ae, \*Corresponding author: irfan.hussain@ku.ac.ae

Binoy Krishna Roy is with the Department of Electrical Engineering, National Institute of Technology Silchar, India. bkrnits@gmail.com  
Bidyadhar Subudhi is with the Department of Electrical Engineering, National Institute of Technology Warangal, India. bidyadharnitrkl@gmail.com

control design of the slow and the fast subsystems. Section V is presented with the results and discussion and Section VI is the conclusion of the paper.

## II. TWO-LINK FLEXIBLE MANIPULATOR DYNAMICS

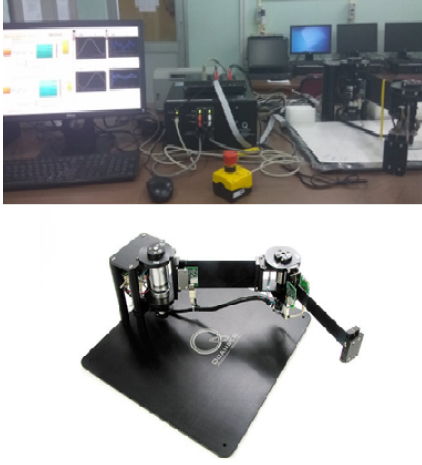


Fig. 1. An experimental set-up of TLFM (two-link flexible manipulator) [12].

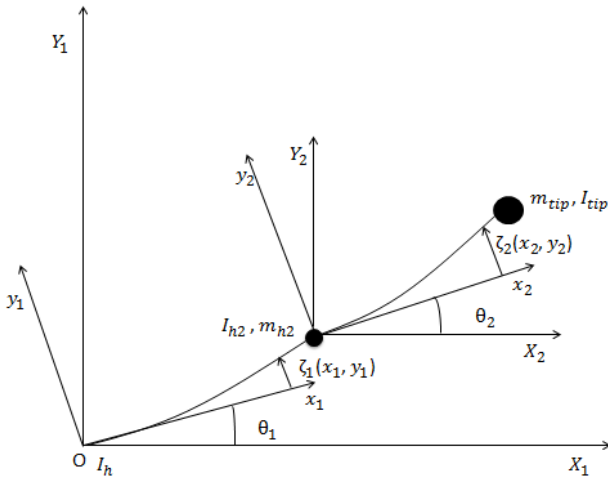


Fig. 2. A schematic representation of the two-link flexible manipulator.

Fig. 2 shows the TLFM system of the Quanser model. The shaft of the motor drives each link in order to track the position desired for link. The AMM model is used for modelling the dynamic model of TLFM.  $(X_j, Y_j)$  represents the inertial frame of the TLFM.  $(x_j, y_j)$  is the moving frame rigid body which is associated with  $j^{th}$  link.  $\tau_j$  expresses the actuated torque at  $j^{th}$  joint,  $\xi_j$  is the deflection of the flexible  $j^{th}$  link. The payload  $m_{tip}$  is attached at the link-2 tip end and  $\theta_j$  is the  $j^{th}$  link joint angle with  $j = 1, 2$ . This method comprises the vibration modes of the dynamics of the flexible link aside from the natural modes. This

flexibility of the link is decomposed for a set of combinations of the eigenfunction modes  $\Phi_{jk}(x_j)$  categorised as mode shapes.  $\delta_{jk}(t)$  is the time dependent generalized coordinate as described in (1). The finite dimensional equation of the flexibility of the links  $\xi_j(x_j, t)$  can be expressed using assumed modes method [2] as

$$\xi_j(x_j, t) = \sum_{k=0}^{r_j} \Phi_{jk}(x_j) \delta_{jk}(t) \quad (1)$$

where at  $x_j (0 \leq x_j \leq l_j)$ , the deflection of the  $j^{th}$  link is considered as  $\xi_j(x_j, t)$ .  $l_j$  as the  $j^{th}$  link length,  $r_j$  as the modes number describing the link's deflection. Also,  $\Phi_{jk}(x_j)$  is the mode function of the  $k^{th}$  mode shape for the link  $j$  bounded to  $k = [1, 2]$ .

Using the approach of Lagrangian, the dynamics of the links are modelled through the energy systems incorporating the AMM modelling. The flexible dynamics is described as given in Lagrangian [2] denoted as below:

$$\frac{d}{dt} \frac{\delta((e_k)_i - (e_p)_i)}{\delta q_i} - \frac{\delta((e_k)_i - (e_p)_i)}{\delta q_i} = \tau_i \quad (2)$$

The time harmonic function is given in (3) for the solution (2)

$$\delta_{jk}(t) = e^{j\omega_{jk}t} \quad (3)$$

and the space eigenfunction as

$$\begin{aligned} \Phi_{jk}(x_j) = & C_{1,jk} \sin(\beta_{jk}x_j) + C_{2,jk} \cos(\beta_{jk}x_j) \\ & + C_{3,jk} \sinh(\beta_{jk}x_j) + C_{4,jk} \cosh(\beta_{jk}x_j) \end{aligned} \quad (4)$$

where in (3),  $\omega_{jk}$  is the  $k^{th}$  natural frequency in angular form of link  $k$  given for the eigenvalue problem,  $\beta_{jk} = \omega_{jk}^2 \rho_i / (EI)_i$ .

Using the mass boundary conditions of the clamped assumptions for the AMM, the clamped boundary conditions using the constants in (4), is given as

$$\begin{aligned} C_{3,jk} &= -C_{1,jk}, \\ C_{4,jk} &= -C_{2,jk} \end{aligned} \quad (5)$$

While the mass condition lead to the homogeneous system in the form

$$[F(\beta_{jk})] \begin{pmatrix} C_{1,jk} \\ C_{2,jk} \end{pmatrix} = 0 \quad (6)$$

This frequency equation can be solved by setting the determinant to zero in (4) and (5). Using (2), the dynamic equation of motion for TLFM with AMM is given as

$$\begin{aligned} M(\theta_j, \delta_j) \begin{pmatrix} \ddot{\theta}_j \\ \ddot{\delta}_j \end{pmatrix} + \begin{pmatrix} h_1(\theta_j, \delta_j, \dot{\theta}_j, \dot{\delta}_j) \\ h_2(\theta_j, \delta_j, \theta_j, \dot{\delta}_j) \end{pmatrix} \\ + K \begin{pmatrix} 0 \\ \delta_j \end{pmatrix} + D \begin{pmatrix} \dot{\theta}_j \\ \dot{\delta}_j \end{pmatrix} = \begin{pmatrix} \tau_j \\ 0 \end{pmatrix} \end{aligned} \quad (7)$$

where  $M$  is the positive definite mass inertia matrix,  $\theta_j$  is the joint angle of the  $j^{th}$  link,  $\delta_j$  is the mode of the  $j^{th}$  link,  $h$ ,  $K$ ,  $D$  and  $\tau$  as the centrifugal and coriolis force, the stiffness matrix, the damping and the input torque, respectively.

### III. SLOW AND FAST SUBSYSTEM VIA SINGULAR PERTURBATION TECHNIQUE

Considering each modes of the flexible links in terms of first and second modes, the manipulator is segregated in two subsystems, a slow and fast dynamics. The dynamic model using two-time scale decomposition method of singular is written as

$$M \begin{pmatrix} \ddot{\theta} \\ \ddot{\delta} \end{pmatrix} + \begin{pmatrix} h_r + D_1\dot{\theta} \\ h_f + D_2\dot{\delta} + K\delta \end{pmatrix} = \begin{pmatrix} I \\ 0 \end{pmatrix} \tau_i \quad (8)$$

This can be further simplified as

$$\begin{cases} \ddot{\theta} = -P_{11}(D_1\dot{\theta} + h_r - P_{12}(h_f + D_2\dot{\delta} + K\delta)) + P_{11}\tau_i \\ \ddot{\delta} = -P_{21}(D_1\dot{\theta} + h_r - P_{22}(h_f + D_2\dot{\delta} + K\delta)) + P_{21}\tau_i \end{cases} \quad (9)$$

where  $\theta_i = [\theta_1 \ \theta_2]^T \in R^2$ : the angular joints,  $\delta_i = [\delta_{i1} \ \delta_{i2}]^T \in R^4$ : the flexible modes of the  $i^{th}$  links for  $i = 1, 2$ ,  $h_r(\theta, \delta) \in R^2$  and  $h_f(\theta, \delta) \in R^4$ : are the terms for gravity, Coriolis and the Centripetal forces,  $D_1 \in R^{2 \times 2}$  and  $D_2 \in R^{4 \times 4}$ : are the damping matrices,  $K \in R^{4 \times 4}$ : the stiffness matrix,  $\tau_i = [\tau_1 \ \tau_2]^T \in R^2$ : the vectors of the input torque. Also, since  $M(\theta, \delta) \in R^{6 \times 6}$  is an inertia matrix of positive definiteness, the inverse exist and can be defined as

$$P = \begin{pmatrix} P_{11} & P_{12} \\ P_{21} & P_{22} \end{pmatrix} = \begin{pmatrix} M_r & M_{rf}^T \\ M_{rf} & M_f \end{pmatrix}^T \quad (10)$$

where  $P_{11} \in R^{2 \times 2}$ ,  $P_{12} \in R^{2 \times 4}$ ,  $P_{21} \in R^{4 \times 2}$ ,  $P_{22} \in R^{4 \times 4}$ . Hence,

$$M_r = [P_{11} - P_{12}P_{22}^{-1}P_{21}]^{-1} \quad (11)$$

Defining a new variable  $\delta = \epsilon x$  and  $K_t = \epsilon K$ , where  $\epsilon$ , the parameter of singular perturbation and defined as  $\frac{1}{\epsilon}$  as the smallest stiffness of  $K$ ,  $K_m = \text{minimum}(K)$ .

Using the new variable, (9) can be rewritten as

$$\ddot{\theta} = -P_{11}(D_1\dot{\theta} + h_r - P_{12}(h_f + D_2\epsilon\dot{x} + K_t x)) + P_{11}\tau_i \quad (12)$$

$$\epsilon\ddot{\delta} = -P_{21}(D_1\dot{\theta} + h_r - P_{22}(h_f + D_2\epsilon\dot{\delta} + K_t x)) + P_{21}\tau_i \quad (13)$$

The control input of the composite structure can be formulated as

$$\tau_i = \tau_s + \tau_f \quad (14)$$

where  $\tau_s$ ,  $\tau_f$  are the slow subsystem and the fast subsystem control input, respectively. Considering the property of two-time scale division with  $\epsilon = 0$  in (13), the slow subsystem for  $x$  can be obtained as

$$\bar{x} = -K_t^{-1}\bar{P}_{22}^{-1}(\bar{P}_{21}\bar{D}_1\dot{\bar{\theta}} + \bar{P}_{21}\bar{h}_1 + \bar{P}_{22}\bar{h}_2 - \bar{P}_{21}\tau_s) \quad (15)$$

where the over-bar term denotes the element for the evaluation with  $\epsilon = 0$ . Substituting (15) in the expression (12), we get

$$\ddot{\bar{\theta}} = (\bar{P}_{11} - \bar{P}_{12}\bar{P}_{22}^{-1}\bar{P}_{21})(-\bar{D}_1\dot{\bar{\theta}} - \bar{h}_r + \tau_s) \quad (16)$$

The above (16) is the TLFM rigid body dynamics for the singularly perturbed system. With (11), the dynamics of slow subsystem is:

$$\ddot{\bar{\theta}} = \bar{M}_r^{-1}(-\bar{D}_1\dot{\bar{\theta}} - \bar{h}_r + \tau_s) \quad (17)$$

Using two-time scale decomposition method, fast subsystem dynamics can be obtained by defining  $\tau = \frac{t}{\sqrt{\epsilon}}$  as the fast time scale and with the boundary correction as

$$\begin{cases} q_1 = x - \bar{x} \\ q_2 = \sqrt{\epsilon}\dot{x} \end{cases} \quad (18)$$

Hence, by using the boundary layer correction term (18), the system can be written as

$$\begin{cases} \frac{dq_1}{d\tau} = q_2 \\ \frac{dq_2}{d\tau} = -P_{21}(D_1\dot{\theta} + h_r) \\ -P_{22}(D_2\epsilon\dot{x} + h_f + K_s x) + P_{21}\tau_i \end{cases} \quad (19)$$

Using time-scale decomposition method, the slow variables can be neglected or treat as the frozen parameter. Hence, pertaining to  $\frac{dq_2}{d\tau} = \sqrt{\epsilon}\dot{x} = 0$ .

Substituting (15) in (19) and setting  $\epsilon = 0$ , yields

$$\frac{dq_2}{d\tau} = -P_{22}K_s q_1 + \bar{P}_{21}\tau_f \quad (20)$$

The fast subsystem dynamics is given in the form as

$$\dot{q} = Q_f q + R_f \tau_f \quad (21)$$

where  $q = [q_1 \ q_2]^T \in R^8$  and

$$Q_f = \begin{pmatrix} 0 & 1 \\ -\bar{P}_{22}K_t & 0 \end{pmatrix}; R_f = \begin{pmatrix} 0 \\ \bar{P}_{21} \end{pmatrix} \quad (22)$$

It corresponds to the linear system of slow parameters of  $\bar{\theta}$ .

### IV. COMPOSITE CONTROL DESIGN

In this section, the composite control input is presented.  $\tau_i = \tau_s + \tau_f$  is the slow and fast control input combination for the flexible manipulator (8). Separate slow and fast subsystems controllers are designed.

#### A. Contraction Theory Tracking Control for Slow Subsystem

Considering the dynamics given in (17)

$$\ddot{\bar{\theta}} = (\bar{M}_r)^{-1}(-\bar{h}_r - \bar{D}_1\dot{\bar{\theta}} + \tau_s) \quad (23)$$

Considering  $y_1 = \bar{\theta}$  and  $y_2 = \dot{\bar{\theta}}$ , (23) can be written as

$$\begin{cases} \dot{y}_1 = y_2 \\ \dot{y}_2 = (\bar{M}_r)^{-1}(-\bar{h}_r - \bar{D}_1 y_2 + \tau_s) \end{cases} \quad (24)$$

The slow subsystem contraction based tracking control design is discussed in two levels:

**Level 1:** The main aim for this level is for tracking the trajectory ( $y_d$ ) desired for the slow dynamics. The trajectory generated from the Genesis-Tesi system [13] is used for tracking the flexible manipulator as given in (45). Hence, the error in the trajectory is defined as  $e_{1s} = y_1 - y_d$ . Considering the derivative of the angular joint as

$$u_1 = y_{2d} = -a_{1s}e_{1s} + \dot{y}_d \quad (25)$$

where  $y_d$  is the differentiable desired trajectory and  $a_{1s} > 0$ . The difference error in the derivative joint variable and desired variable is given as:

$$x_{1s} = y_2 - u_1 = y_2 + a_{1s}e_{1s} - \dot{y}_d \quad (26)$$

Then, the dynamics is given as

$$\dot{x}_{1s} = \dot{y}_2 + a_1 \dot{e}_{1s} = (\bar{M}_r)^{-1}(-\bar{h}_r - \bar{D}_1 y_2 + \tau_s) + a_1 \dot{e}_{1s} \quad (27)$$

**Level 2:** By considering the input control of the slow dynamics (28), the control inputs will be obtained to stabilize  $e_{1s}$  and  $x_{1s}$  in this step.

$$\tau_s = \bar{M}_r(\bar{h}_r + \bar{D}_1 y_2 - a_{1s} \dot{e}_{1s} - a_{2s} x_1 - e_{1s}) \quad (28)$$

Hence, the dynamics of  $x_{1s}$  is given as

$$\dot{x}_{1s} = -a_{2s} x_1 - e_{1s} \quad (29)$$

Thus, the error dynamics in the transform domain is given as

$$\begin{cases} \dot{e}_{1s} = x_1 - a_{1s} e_1 \\ \dot{x}_{1s} = -a_{2s} x_1 - e_{1s} \end{cases} \quad (30)$$

**Theorem 1:** A section of state space is regarded as a contracting zone for the equation (8) of a dynamical system if the differential  $\frac{\delta(x,t)}{\delta x}$  of that region is uniformly negative definite (UND) [13]. By UND, with  $\gamma > 0, \forall(x,t) > 0$  and  $\frac{\delta(x,t)}{\delta x} \leq -\gamma I$ , there exist  $J_s = \frac{1}{2}[\frac{\delta(x,t)}{\delta x} + (\frac{\delta(x,t)}{\delta x})^T] \leq -\gamma I < 0$ .

By using the Theorem 1, for all the condition of contraction theory, the overall transformed dynamics is given in (30). Hence, this is for the uniformly negative definite closed loop system. Hence, Jacobian matrix of (30) is given as

$$J_{1s} = \begin{pmatrix} a_{1s} & 1 \\ -1 & a_{2s} \end{pmatrix} \quad (31)$$

The symmetric part of (31) is obtained as

$$-J_s = -\frac{1}{2}(J_{1s} + J_{1s}^T) = \begin{pmatrix} a_{1s} & 0 \\ 0 & a_{2s} \end{pmatrix} \quad (32)$$

The closed loop error of the Jacobian matrix as in (31) and (32), is UND when  $a_{1s}$  and  $a_{2s}$  are chosen as a quantity which is positive. Using the property of Theorem 1, the angular joint follows (45) and gives the stable closed loop system dynamics.

### B. Backstepping Control for Fast Subsystem

This stage, comprises the fast subsystem backstepping controller design for the quick tip deflection. From (30) and (31), considering  $z = q$ , (21) is rewritten as

$$\begin{cases} \dot{z}_1 = z_2 \\ \dot{z}_2 = -Q_f z_1 + R_f \tau_f \end{cases} \quad (33)$$

where  $Q_f = \bar{P}_{22} K_t$  and  $R_f = \bar{P}_{21}$ . The links error deflection are obtained as

$$\begin{cases} e_{1f} = z_d - z_1 \\ e_{2f} = v_d - z_2 \end{cases} \quad (34)$$

Here,  $z_d$  is the desired link deflection and twice differentiable for the flexible manipulator and  $v_d$  is the virtual control term. The error dynamics is obtained as

$$\begin{cases} \dot{e}_{1f} = \dot{z}_d - \dot{z}_1 \\ \dot{e}_{2f} = \dot{v}_d + Q_f z_1 - R_f \tau_f \end{cases} \quad (35)$$

Using Theorem 2, backstepping control law is calculated and designed for the suppression of tip deflection.

**Theorem 2:** Supposing that the control law obtained by backstepping in (36) with the error dynamics (35) controls the fast dynamics of the subsystem given in (33), hence, the system follows the desired tip deflection  $z_d$ .

$$\tau_f = (R_f)^{-1}(\dot{v}_d + Q_f z_1 + a_{1b} e_{2f}) \quad (36)$$

**Proof:** A backstepping controller is designed in this step for (33).

**Level 1:** Taking the candidate of Lyapunov function as

$$v_{1f} = \frac{1}{2} e_{1f}^2 \quad (37)$$

The derivative of (37) using (35) is

$$\dot{v}_{1f} \begin{cases} = e_{1f}(\dot{z}_d + e_{2f} - v_d) \\ = e_{1f}\dot{z}_d - e_{1f}v_d + e_{1f}e_{2f} \end{cases} \quad (38)$$

The virtual control variable  $v_d$  selected for the derivative of Lyapunov function (38) for the negative definiteness is given as

$$v_d = \dot{z}_d + A_1 e_{1f} + e_{2f} \quad (39)$$

where  $A_1$  is the positive definite matrix.

The derivative of (38) can be given as

$$\dot{v}_{1f} = -A_1 e_{1f}^2 \quad (40)$$

From (40), it is noted as a negative definite function. Hence,  $z_1$  in (33), the first variable is stabilized.

**Level 2:** In this step, the next state variable for backstepping control is designed for its stability. Also,  $\tau_f$ , the fast subsystem control input is designed.

Taking the Lyapunov function candidate as

$$v_2 = v_1 + \frac{1}{2} e_{2f}^2 \quad (41)$$

Using the second error variable (38), the time derivative (40) is

$$\dot{v}_{2f} = -A_1 e_{1f}^2 + e_{2f}(\dot{v}_d + Q_f z_1 - R_f \tau_f) \quad (42)$$

It can be seen from (42) that, if the input torque  $\tau_f$  is selected as (43), it is negative definite.

$$\tau_f = (R_f)^{-1}(\dot{v}_d + Q_f z_1 + A_2 e_{2f}) \quad (43)$$

Using the input torque of  $\tau_f$  defined in (43), the derivative in (42) can be rewritten as

$$\dot{v}_2 = -(A_1 e_{1f}^2 + A_2 e_{2f}^2) \quad (44)$$

Hence, from the theory of Lyapunov stability, (44) is a negative definite function such that it requires the condition of  $A_1, A_2$  as the positive constant matrices. Also,  $e_{1f}$  and  $e_{2f}$ , the error variables are asymptotically stable. Thus, the proper selection of the parameters of  $A_1$  and  $A_2$  leads to the fast suppression and quick stabilization of the error variables leading it to zero. Fig. 3 depicts the composite control schematic diagram of the singular perturbation TLFM.

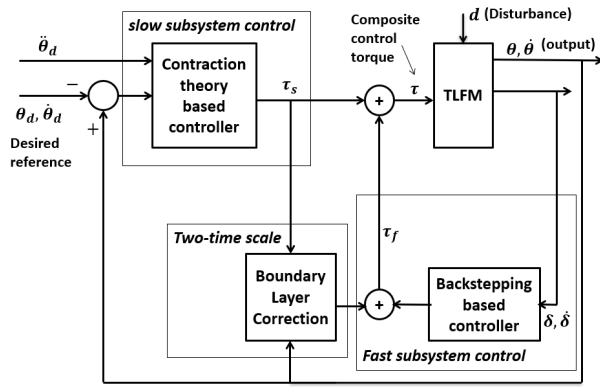


Fig. 3. Composite control model using singular perturbation for a TLFM.

### V. RESULTS AND DISCUSSION

Using fourth-order Runge-kutta method with a step time  $h = 10^{-3}$  in MATLAB, the dynamics of the robotic manipulator is solved. The dynamics of the desired trajectory [13] is given as below:

$$\begin{cases} \dot{y}_1 = y_2 \\ \dot{y}_2 = y_3 \\ \dot{y}_3 = p_3 y_3 + p_2 y_2 + p_1 y_1 + y_1^2 \end{cases} \quad (45)$$

where  $p_1 = -1.1$ ,  $p_2 = -1.2$ ,  $p_3 = -0.50$  are the parameters and  $y_1, y_2, y_3$  are the states of the chaotic behaviour of the system (45). Hence, with the desired trajectories:  $y_d = y_1, \dot{y}_d = y_2$  and  $\ddot{y}_d = y_3$ . The initial condition of  $y(0) = [0.1, 0.1, 0.002]^T$  are chosen for the chaotic system (45).

The chaotic system (45) time responses and chaotic attractors are shown in Fig. 4 and Fig. 5. Table I gives the physical parameters involved in the model design of Quanser two-link FM (8) for n-dimensional discretized system from [12].

Also,  $[\theta(0)] = [0.1, 0.1]^T$ ;  $[\delta(0)] = [0.0, 0.0, 0.0, 0.0]^T$  are

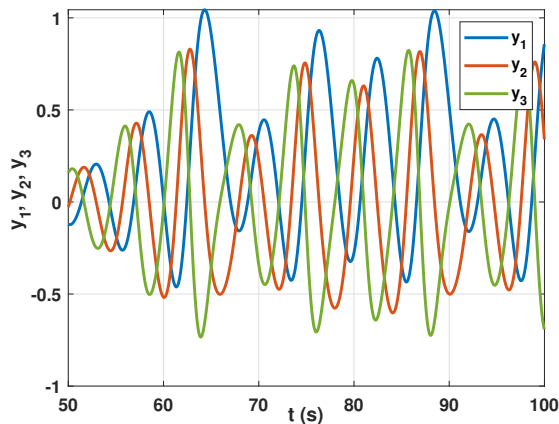


Fig. 4. Time response of the desired trajectories for the dynamics (45) of slow subsystem.

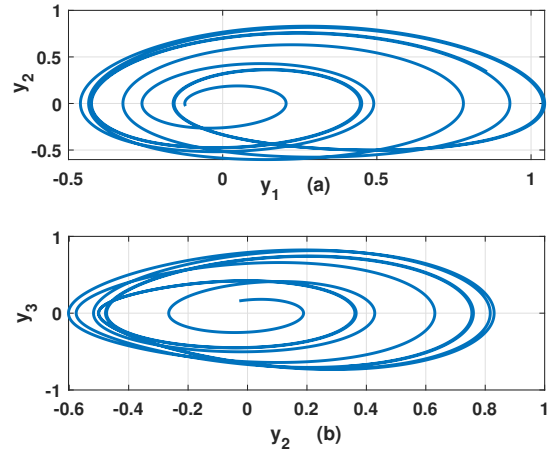


Fig. 5. The chaotic attractor of (45): (i) on  $y_1 - y_2$  plane and (ii) on  $y_2 - y_3$  plane.

TABLE I

THE PHYSICAL PARAMETERS OF THE QUANSER TWO-LINK FLEXIBLE MANIPULATORS [12].

Parameters	Values	Units
Mass of link-1, $M_1$	0.15268	kg
Mass of link-2, $M_2$	0.0535	kg
Mass of hub joint-2, $m_{h2}$	0.689	kg
Tip payload mass, $M_{tip}$	0.145	kg
Length of link-1, $L_1$	0.202	m
Length of link-2, $L_2$	0.2018	m
Link-1 armature resistance, $R_{m1}$	11.5	$\Omega$
Link-2 armature resistance, $R_{m2}$	2.32	$\Omega$
At load, link-1, $I_h$ equivalent moment of inertia	0.099	$kgm^2$
At load, link-2, $I_{h2}$ equivalent moment of inertia	0.092	$kgm^2$
Link-1 moment of inertia, $I_{l1}$	0.002035	$kgm^2$
Link-2 moment of inertia, $I_{l2}$	0.0007204	$kgm^2$
Link-1 Viscous, $B_{eq1}$ coefficient of damping	4	$Nms/rad$
Link-2 Viscous, $B_{eq2}$ coefficient of damping	1.5	$Nms/rad$
Link-1 gear box efficiency, $\eta_{g1}$	0.85	
Link-2 gear box efficiency, $\eta_{g2}$	0.9	
Link-1, Link-2 motor efficiency, $\eta_{m1}, \eta_{m2}$	0.85	
Link-1 back e.m.f. constants, $K_{m1}$	0.119	V/rad
Link-2 back e.m.f. constants, $K_{m2}$	0.0234	V/rad
Link-1 gear ratio, $K_{g1}$	100	
Link-2 gear ratio, $K_{g2}$	50	
Link-1 motor torque constants, $K_{t1}$	0.119	Nm/A
Link-2 motor torque constants, $K_{t2}$	0.0234	Nm/A
Link-1 stiffness constants, $K_{stiff1}$	22	Nm/rad
Link-2 stiffness constants, $K_{stiff2}$	2.5	Nm/rad

the initial conditions of terms in (8). The gains used in contraction based theory for  $a_{1s}$  and  $a_{2s}$  are given as:

$$a_{1s} = \begin{pmatrix} 3 & 0 \\ 0 & 3 \end{pmatrix}; a_{2s} = \begin{pmatrix} 9 & 0 \\ 0 & 9 \end{pmatrix}$$

Gains values used in the backstepping controller are given as:  $A_1 = 6I_{4 \times 4}$ ,  $A_2 = 9I_{4 \times 4}$ . The gains are chosen such that it achieves good tracking performances with lesser control efforts.

The chaotic trajectory tracking  $\theta_i$  of the TLFM with

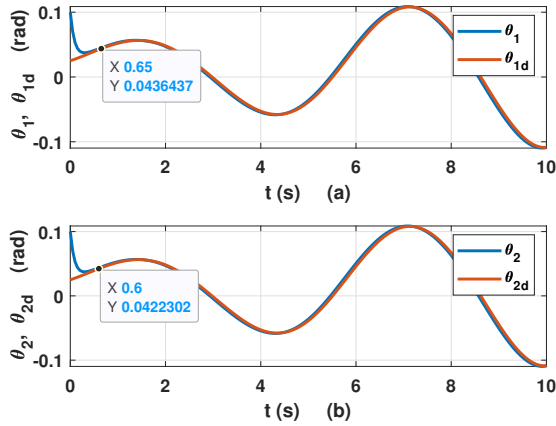


Fig. 6. Trajectory tracking of chaotic path for link-1 and link-2 of the TLFM (45).

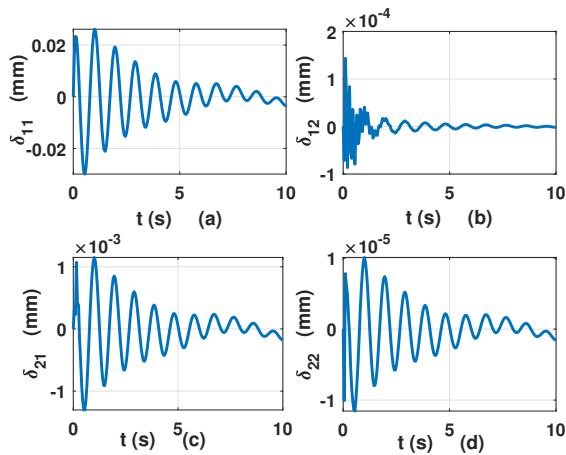


Fig. 7. a) Link-1 first mode, b) Link-1 second mode, c) Link-2 first mode and d) link-2 second mode of tip deflection using (21).

tip payload mass of 0.145 kg for a control torque of  $\tau_{si}$  in the links 1 and 2 are shown in Fig. 6. The trajectory of the designed controller tracks the Genesio-Tesi chaotic desired signal and converge at 0.65 s for link-1 and 0.6 s for link-2. The tip deflection first and second modes of link 1, 2 are depicted in Fig. 7. In comparison, the vibration is larger in the first mode of the first link, but it decreases to  $10^{-3}$  in the first mode of the second link. In comparison to the link-1 first

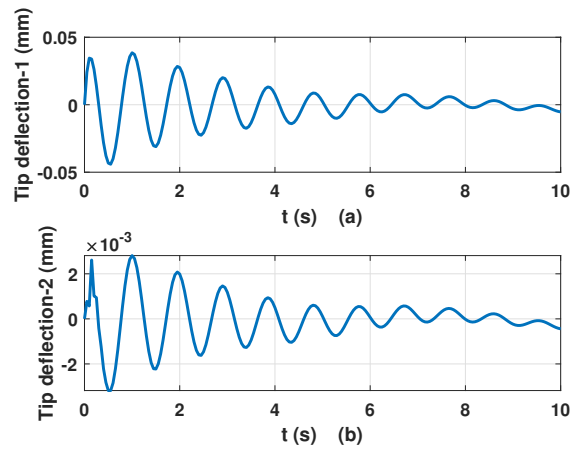


Fig. 8. Tip deflection for link-1 (combination of modes-1 and 2) and link-2 (combination of modes-1 and 2) using (21).

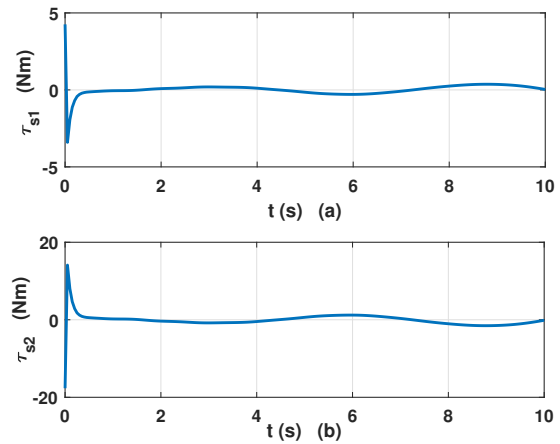


Fig. 9. Control inputs behaviour of the slow subsystem during the trajectory tracking with using (28).

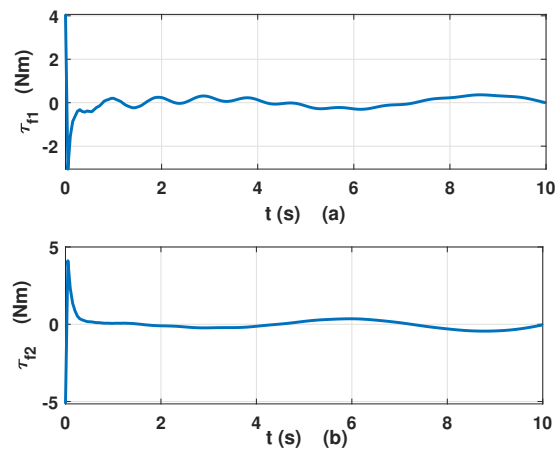


Fig. 10. Control inputs behaviour of the fast subsystem during the trajectory tracking using (43).

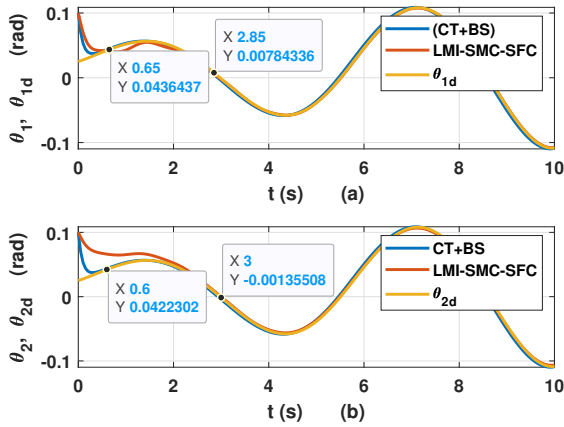


Fig. 11. Chaotic path trajectory tracking comparison for link-1 and link-2 using CT+BS and with LMI-SMC-SFC [14].

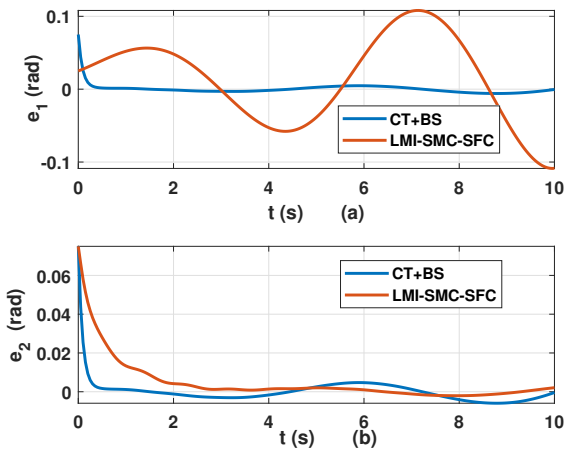


Fig. 12. Trajectory tracking error comparison for both the links using CT+BS and with LMI-SMC-SFC [14].

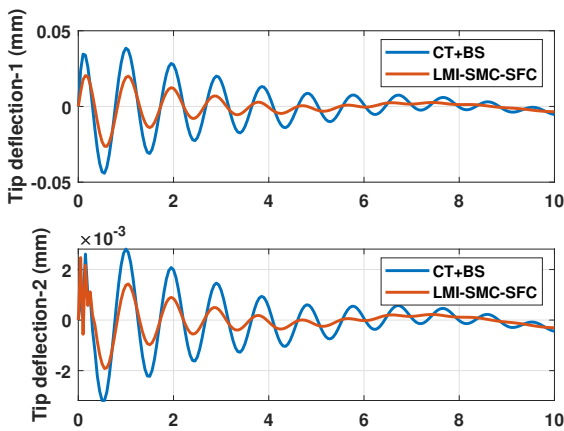


Fig. 13. Tip deflection error comparison for both the links using CT+BS and LMI-SMC-SFC [14].

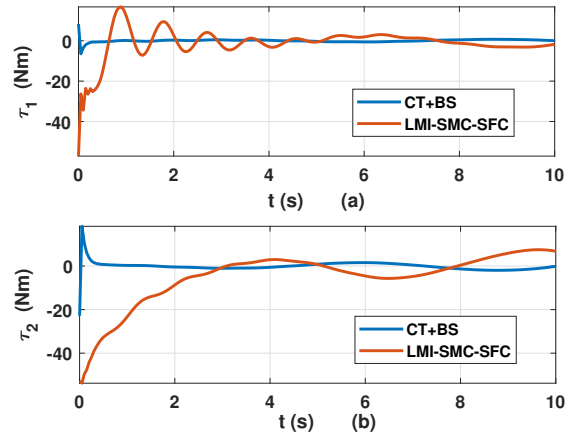


Fig. 14. Comparison of the control inputs for both the links using CT+BS and LMI-SMC-SFC [14].

mode and link-2 first mode, the modes of vibration in the second mode reduces significantly owing to the combination of the modes mapping to the total tip deflection, as shown in Fig. 8. As this is a chaotic trajectory, the vibration settles down but within a range of  $-0.02$  mm to  $+0.02$  mm in the trajectory tracking of tip deflection vibration suppression. At the initiation of the second link motion, vibration is because of the first link's inertia. It is also shown that the link modes are suppressed within a minimal zero value. The slow subsystem control inputs  $\tau_{s1}$  and  $\tau_2$  of the link-1 and link-2 are given in Fig. 9. It is seen that the control torque of slow subsystem is in the range of  $+8.323$  Nm to  $-6.461$  Nm for the link-1 and  $+18.223$  Nm to  $-22.813$  Nm for link-2. Fig. 10 shows the fast control torque of the subsystem in the range of  $+4.065$  Nm to  $-3.055$  Nm for link-1,  $+4.110$  Nm to  $-5.150$  Nm for the tip deflection suppression. The combination of slow and fast subsystem controllers gives the final control inputs.

A comparative simulation is done with the existing controller in the literature [14]. Fig. 11 shows the trajectory tracking of both the controllers along with the chaotic trajectory. In our designed composite controller of contraction theory and backstepping (CT+BS), the trajectory converged at  $0.654$  s for link-1 and  $0.6$  s for link-2. In comparison with the existing controller (LMI-SMC-SFC) of [14], the trajectory converged at  $2.85$  s for link-1 and  $3$  s for link-2. The comparative joint trajectory tracking error of link-1 and link-2 of both the controllers are shown in Fig. 12. As seen from Figs. 11 and 12, links 1, 2 reach the desired position faster in the designed controller than the existing controller. So, each of the links of the flexible manipulator is able to track the desired trajectory in the form of Genesis-Tesi chaotic trajectory.

The comparative analysis of the tip deflection of designed and the existing controllers of links 1, 2 are shown in Fig. 13. In this figure, the tip deflection vibrates higher in magnitude for the designed controller with a value of  $+0.02$  mm for the

link-1 and  $+1 \times 10^{-3}$  mm for link-2 in the first and the second overshoot which then comparatively reduces to almost zero. Apparently, Fig. 14 shows the comparison of the composite control inputs in terms of the combination of slow and fast subsystems for link-1 and link-2. Fig. 14 depicts that the designed composite controller torque range is  $-6.461$  Nm to  $+8.323$  Nm for link-1 and  $-22.813$  Nm to  $+18.223$  Nm. While the existing controller has the control torque range of  $-57.140$  Nm to  $+16.784$  Nm for the link-1 and  $-52.822$  Nm to  $+2.94664$  Nm. It is also seen from Fig. 14 that the magnitudes of the combination of the proposed controllers of fast subsystem and slow subsystem are much lesser than that reported one in [14]. It is clear from all the comparisons that the proposed composite controller tracks the trajectory more quickly while requiring fewer control inputs and better vibration suppression.

## VI. CONCLUSION

The singular perturbation assumed modes method is used in this research to produce the Quanser two-link flexible manipulator discretized  $n$ -dimensional model. This realizes the segregation of two subsystems: a fast and a slow, facilitating the dynamic complexity and the separate design of the controllers for both the subsystems. In this paper, the slow subsystem is controlled using a contraction-based controller, and the fast subsystem is controlled using a backstepping controller. The required tracking is achieved using contraction theory based composite control and backstepping control for the deflection suppression of the two-link flexible manipulator. The results indicate the robustness and the effectiveness of the designed two-time scale controller for the desired trajectory tracking system. The designed composite controller exhibits better performance in terms of fast tracking time, quicker tip suppression deflection and lesser control inputs. The experimental validation of the proposed composite controller in the presence of disturbances and uncertainties can be future direction of this work.

## VII. ACKNOWLEDGEMENTS

This research is supported by ASPIRE, the technology program management pillar of Abu Dhabi's Advanced Technology Research Council (ATRC), under the ASPIRE project "Aspire Research Institute for Food Security in the Drylands" within Theme 1.4 and by the KU Center for Autonomous Robotic Systems - Khalifa University of Science and Technology under Award No. RC1-2018-KUCARS.

## REFERENCES

- [1] X. Zhang, W. Xu and V.S. Chellaboina, "PDE Modeling and Control of a Flexible Two-Link Manipulator," *IEEE Transactions on Control Systems Technology*, vol. 13, pp. 123–126, 2005.
- [2] S. K. Pradhan and B. Subudhi, "Nonlinear Adaptive Model Predictive Controller for a Flexible Manipulator: An Experimental Study," *IEEE Transactions on Control Systems Technology*, vol. 22, pp. 770–778, 2014.
- [3] J. R. Forbes and C. J. Damaren, "Design of Optimal Strictly Positive Real controllers using Numerical Optimization for the Control of Flexible Robotic Systems," *Journal of the Franklin Institute*, vol. 348, pp. 2191–2215, 2011.
- [4] K. Lochan, B. K. Roy and B. Subudhi, "SMC Controlled Chaotic Trajectory Tracking of Two-link Flexible Manipulator with PID Sliding Surface," *IEEE Transactions on Control Systems Technology*, vol. 22, pp. 770–778, 2014.
- [5] M. Korayem and M. Haghpanahi, "Finite Element Method and Optimal Control Theory for Path Planning of Elastic Manipulators," *New Adv. Intell. Decis. Technol.*, vol. 199, pp. 117–126, 2009.
- [6] S. H. Lee and C. W. Lee, "Hybrid Control Scheme for Robust Tracking of Two-link Flexible Manipulator," *J. Intell. Robot. Syst.*, vol. 34, pp. 431–452, 2002.
- [7] Y. Li, G. Liu, T. Hong and K. Liu, "Robust Control of a Two-link Flexible Manipulator with Quasi-static Deflection Compensation using Neural Networks," *J. Intell. Robot. Syst.*, vol. 44, pp. 263–276, 2005.
- [8] A. Khorrami, F. Jain and S. Tzes, "Experiments on Rigid Body-Based Controllers with Input Preshaping for a Two-Link Flexible Manipulator," *IEEE Trans. Robot. Autom.*, vol. 10, pp. 55–65, 1994.
- [9] Y. Wang, Y. Feng and X. Yu, "Fuzzy Terminal Sliding Mode control of Two-link Flexible Manipulators," in: *34th IEEE Annu. Conf. Ind. Electron.*, pp. 1620–1625, 2008.
- [10] M. Ashayeri and A. Farid, "Trajectory Tracking for Two-Link Flexible Arm via Two-Time Scale and Boundary Control Methods," in: *Proc. IMECE2008 2008 ASME Int. Mech. Eng. Congr. Expo.*, pp. 1–9, 2008.
- [11] B. Subudhi and A.S. Morris, "Dynamic Modelling, Simulation and Control of a Manipulator with Flexible Links and Joints," *Rob. Auton. Syst.*, vol. 41, pp. 257–270, 2002.
- [12] QUANSER, Equation for the First (second) Stage of the 2DOF serial Flexible Link Robot, 2006.
- [13] W. Lohmiller and J. E. Slotine, "On Contraction Analysis for Nonlinear Systems," *Automatica*, 31(3) pp. 1-27, 1996.
- [14] K. Lochan, R. Dey, B. K. Roy and B. Subudhi, "Tracking Control with Vibration Suppression of a Two-link Flexible Manipulator using Singular Perturbation," *Proceedings of the 8th International Workshop Soft Computing Applications (SOFA 2018)*, Vol. I, pp. 365–377, 2017.